Effect of Cyclic Fatigue on Static Fracture Loads in ProTaper Nickel-Titanium Rotary Instruments

Cheryl J. Ullmann, cand med dent, Ove A. Peters, PD, Dr med dent, MS FICD

Abstract

The aim of the present study was to evaluate static fracture loads of ProTaper Nickel-Titanium instruments that had been subjected to various degrees of cyclic fatigue. Torque and angle at failure of new instruments and instruments that had been stressed to 30, 60, or 90% of their cyclic fatigue rotations in a simulated canal (90° and 5 mm radius) were tested according to ISO 3630-1. With unused ProTaper instruments, resistance to cyclic fatigue decreased with diameter increase and ranged from 158 to 450 rotations. Torque at failure ranged from 0.5 to 2.1 Ncm and showed a strong linear relationship to instrument diameter ($r^2 = 0.9$) while angle at failure was weakly related to diameter ($r^2 = 0.46$). Cyclic prestressing significantly reduced torsional resistance in finishing files, while shaping files were largely unaffected. In conclusion, build-up of tension within NiTi rotary instruments depends on instrument diameter. Clinically, larger instruments that have been subjected to some cyclic fatigue should be used with great care or discarded.

From the Department of Preventive Dentistry, Division of Endodontology, Periodontology and Cariology, University of Zürich, Zürich, Switzerland and the Department of Preventive and Restorative Dental Sciences, Endodontic Division, University of California San Francisco, San Francisco, CA.

Address request for reprints to Dr. Ove Peters, Department of Preventive Dentistry, Periodontology and Cariology, University of Zürich, Plattenstr. 11, CH-8028 Zürich, Switzerland; E-mail address: ove.peters@zzmk.unizh.ch.

While it is generally agreed that Nickel-Titanium (NiTi) rotary instruments help to prepare root canals with few or no procedural errors, there is also an increased likelihood of instrument separation compared to hand instruments (1–3), which may ultimately lower healing probabilities (4).

Two distinct separation mechanisms were described by Sattapan et al. (5) in routinely discarded Quantec (Analytic Endodontics, Glendora, CA) rotary files: torsional (ductile) and fatigue (brittle) fracture. Instruments fractured because of torsional loads often carried specific signs such as plastic deformation, while instruments separated because of fatigue exhibited no specific patterns in light microscopic observations (5). Similar results were obtained by Luebke et al. (6) regarding stainless steel Gates Glidden drills.

Instruments used clinically will be subjected to both fatigue and torsional load simultaneously, possibly resulting in instrument separation because of hybrid forces (7). The actual contribution of torsional load and cyclic fatigue to potential instrument separation may be dependent on cross-sectional instrument design and the distribution of forces within the instruments (8).

Gambarini (7) found that the use of a torque-controlled motor, and consequently less torque during instrumentation, significantly reduced cyclic fatigue for selected ProFile.04 and .06 instruments. However, Yared et al. (9) reported that clinical use by a trained endodontist did not decrease the numbers of rotations of ProFile .06 files resulting in breakage. Moreover, recent reports indicated that K3 instruments (SybronEndo, West Collins, CA) had lower torsional resistance after they were used to shape canals in plastic blocks (10, 11). Hence, an impact of torsional loads on cyclic fatigue lifespans and vice versa is controversial.

Therefore, the aim of the present in vitro study was to evaluate static fracture loads of NiTi rotary instruments that had been stressed to various degrees of cyclic fatigue.

Materials and Methods

New sets of ProTaper rotary instruments (Fig. 1, Dentsply-Maillefer, Ballaigues, Switzerland) were used in this study, consisting of six individual rotaries (Shaper X, shaping files 1 and 2, finishing files 1, 2, and 3).

Instrument prestressing and determination of fracture loads according to ISO 3630-1 (12) were done using a special torque testing platform that is described in detail elsewhere (2). Briefly, for the determination of resistance to cyclic fatigue, unused instruments ($n = 8$ in each group) were placed in a stainless steel root canal phantom with 5 mm radius and 90° curve (2, 13); the instruments were then rotated at 250 rpm until fracture occurred to determine baseline scores (see Table 1). Time to fracture was noted to the nearest 0.1 s and numbers of rotations to fracture calculated. Pilot experiments had indicated that lubrication with various agents did not result in different cyclic fatigue scores but helped to reduce heat generated in the steel phantom. Consequently, a silicone-based lubricant was used (Motorex 622, Bucher, Langenthal, Switzerland).

Further groups of instruments were then prestressed to 30, 60, and 90%, respectively, of the numbers of rotations previously determined as cyclic fatigue scores.

Static fracture loads were determined for new and prestressed rotary instruments according to ISO 3630-1 (12): 3 mm of the file tips were secured firmly in a specifically designed soft brass holder. The instruments' shank was then rotated at 2 rpm until fractures occurred. Care was taken to adjust instruments into the holder so that no tension or deflection was present before testing.

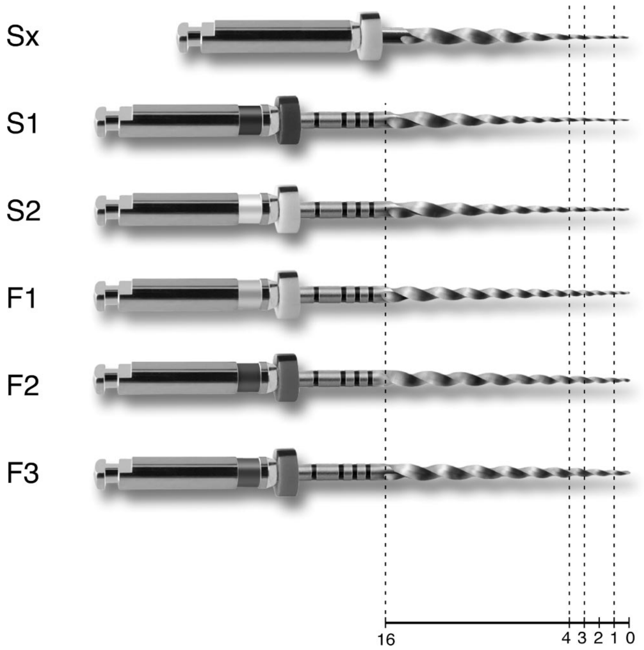

Figure 1. Schematic diagram of ProTaper instruments (Sx: Shaper X; S1 and S2: shaping files 1 and 2; F 1-3: finishing fines 1-3). Bar at bottom illustrates measurements along working section of the instruments. Diameters at respective points are termed D1, D3, D4, to D16.

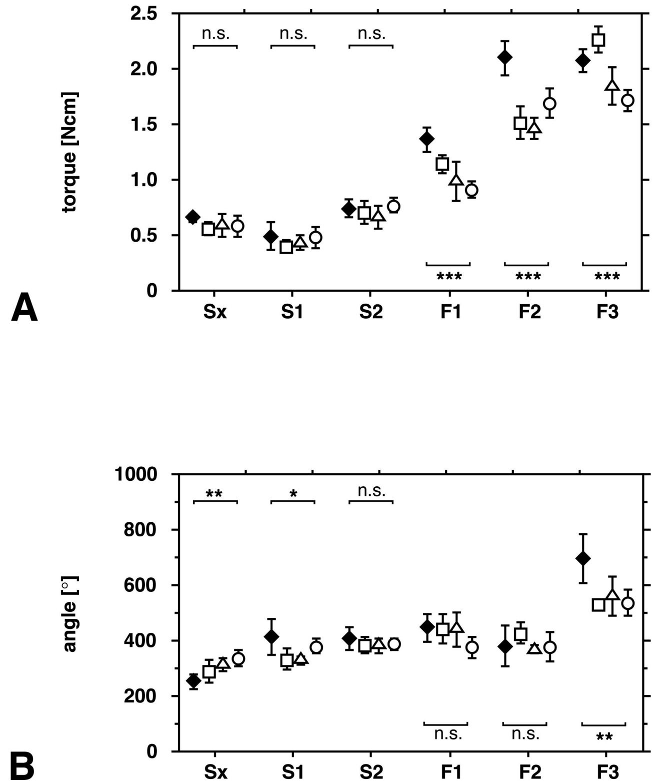

Figure 2. Torque (*A*) and angle (*B*) at failure for new (◆) and prestressed ProTaper instruments. Stressing was done in a stainless steel root canal phantom with 30% (□), 60% (△), and 90% (○) of the numbers of rotations required for fatigue failure ($p < 0.001$; $n = 8$ in each group).

Torque and angle of rotation were continuously measured with a memocouple (MTTRA 2, with amplifier Microtest, both Microtec Systems, Villingen, Germany), digitized at 100 Hz (PCI-MIO-16XE, National Instruments, Austin, TX) and fed into a computer (G3 Power Mac, Apple, Cupertino, CA). Torque and angle at failure were calculated offline from the original records and tabulated.

Instrument fragments were prepared for scanning electron microscopy and photographed at magnifications between 50 and 1000× (Amray 1810, Cambridge, MA).

Data were normally distributed and consequently, statistical analysis was done by parametric procedures. Torque and angle at failure for unused instruments were compared to shaft diameters with Pearson correlation coefficients. One-way analysis of variance and Scheffè posthoc tests at $\alpha = 0.05$ (StatView 4.5, Abacus Concepts, Berkeley, CA) were used to evaluate the effect of prestressing. Torque and angle at fracture were dependent variables while instrument type and prestress levels were independent measures.

Results

Table 1 lists baseline torque and angle at failure for unused ProTaper instruments subjected to torsional loads according to ISO 3630-1. Finishing instruments (F1-3) were significantly more resistant to torque than shaping instruments (Sx, S1, S2). Torque at failure increased from F1 to F2 and F3, while Sx and S2 were more resistant to torque than S1. When torque at failure was correlated to instrument diameter at D3, a significant relationship was found ($p < 0.001$, $r^2 = 0.90$).

Angle at failure was statistically similar among unused ProTaper instruments. An exception to this pattern was F3 that fractured at a significantly greater angle ($p < 0.05$; Table 1). Rotations to fracture because of cyclic fatigue decreased with increasing instrument size (Table 1) with F3 separation occurring significantly earlier than with the other files ($p < 0.01$). When angle at failure was correlated to instrument diameter at D3, a significant but weak relationship was found ($p < 0.01$, $r^2 = 0.46$).

During prestressing with cyclic fatigue loads of 30, 60, and 90% a total of 12 out of 156 instruments separated before the designated

TABLE 1. Baseline scores for unused ProTaper instruments: torque and angle at failure as well as fatigue lifespan. Diameters* at D3 in mm are shown in parentheses

	Torque [Ncm]	Angle [°]	Rotations [*n*]
Shaper X (0.325)	0.67 ± 0.04	256 ± 28	158 ± 35
Shaping file 1 (0.275)	0.51 ± 0.13	416 ± 65	450 ± 83
Shaping file 2 (0.335)	0.76 ± 0.08	412 ± 43	398 ± 64
Finishing file 1 (0.410)	1.38 ± 0.11	451 ± 51	385 ± 38
Finishing file 2 (0.490)	2.11 ± 0.15	384 ± 72	346 ± 40
Finishing file 3 (0.570)	2.09 ± 0.11	701 ± 90	166 ± 44

* Data according to the manufacturer.

$N = 8$ in each group.

Differences in torque, angle and rotation at failure between files were overall significant (ANOVA, $p < 0.001$).

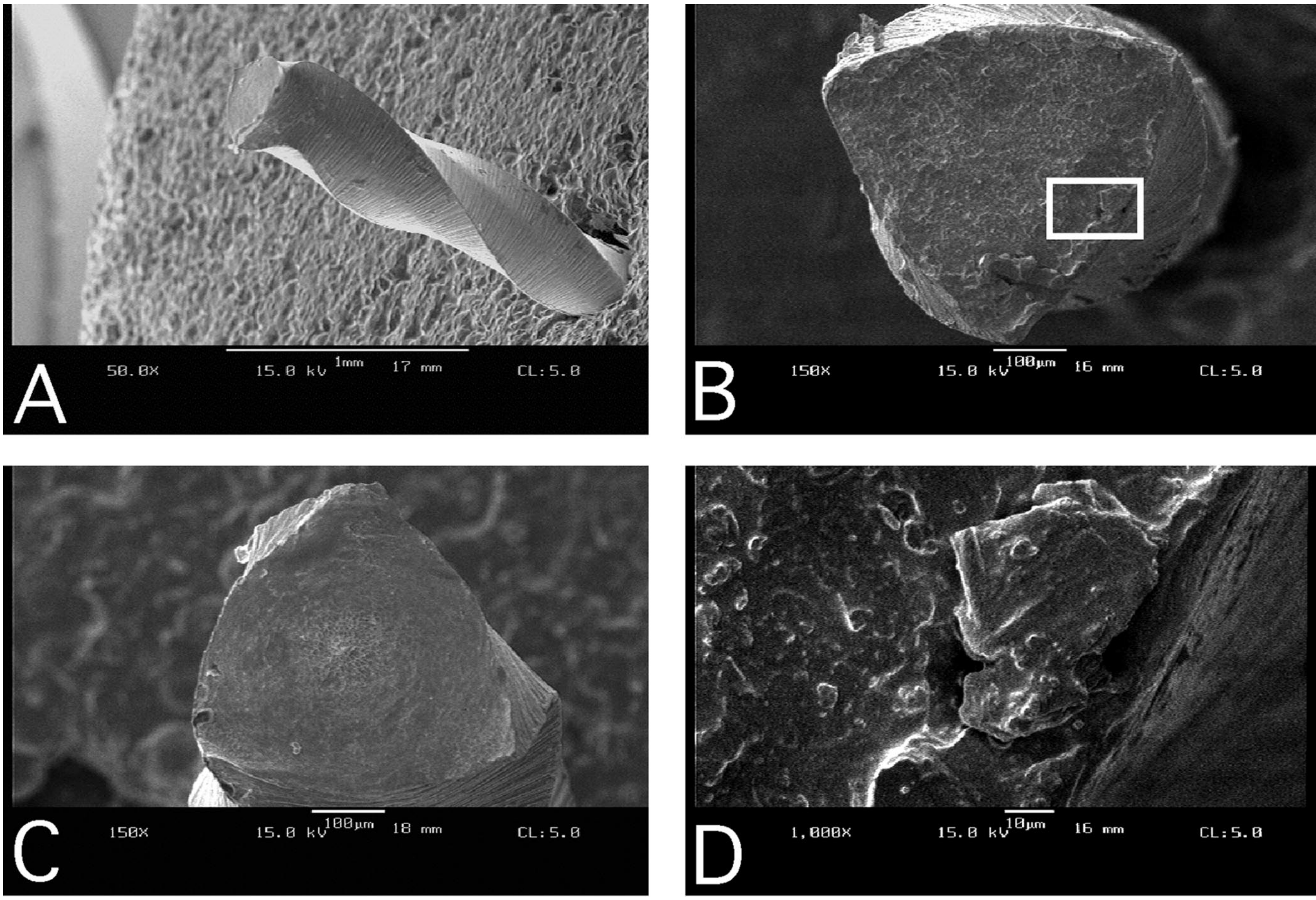

Figure 3. Scanning electron micrographs of ProTaper F1 instruments after separation. (*A*, *C*) Deformation and separation because of torsional loading (original magnifications 50× and 150×). (*B*, *D*) Separation because of cyclic fatigue with typical signs of crack initiation (white area in *B* and shown in *D*, orig. magnifications 150× and 1000×, respectively).

numbers of rotations were reached. Figure 2 shows the effect of prestressing on instrument behavior under torsional load. ANOVAs indicated significant effects of instrument size and stress levels on torque and angle at failure ($p < 0.001$, Fig. 2). However, various instruments reacted differently to prestressing. While torsional resistance for both S1 and S2 was unaltered, torques to failure decreased significantly for F1, F2, and F3. Angles at failure for finishing instruments 1 and 2 did not change significantly because of cyclic prestressing; however, F3 had reduced angles at failure already after presstressing with 30% cyclic fatigue load.

Scanning electron micrographs revealed two distinct fracture patterns shown in Fig. 3: torsional fracture and fatigue fracture. Torsional fracture was characterized by plastic deformation (Fig. 3*A*) and a pattern of lines near the center of rotation (Fig. 3*C*) while fatigue fracture had a more homogenous appearance with striations (Fig. 3*B*) and areas of crack initiation (Fig. 3D). Prestressing did not alter torsional fracture patterns compared to unstressed files for any of the tested instruments.

Discussion

Fracture mechanisms of rotary NiTi instruments are of interest clinically not only because instrument separation may theoretically impair clinical outcomes (14), but also because clinicians are apprehensive of procedural mishaps (15).

Engine-driven instruments can and will fracture clinically when subjected to suprathreshold torque (1, 2, 5, 16). However, work hardening from repetitive loading has been also cited as a reason for instrument separation, in particular for instruments with greater diameter (5). Cyclic loading with tension and compression zones leads to crack propagation originating from manufacturing flaws that function as initial crack nuclei (17). A build-up of stresses, torsional and flexural, might occur clinically, specifically for re-used instruments. The relative contribution of torsional and flexural stress as well as the overall effect on torsional resistance of NiTi instruments is unclear. Hence, the design of the present study attempted to simulate the effect of flexural stress on torsional resistance.

When torques at failure of unused ProTaper instruments are compared, it is necessary to group instruments according to their diameter at D3 (see Fig. 1), where testing according to ISO 3630-1 is done (12). This is because ProTaper instruments differ from other NiTi rotary instruments in that they have variable tapers along their shafts and consequently no linear increase in diameters at D3 (Table 1). In accordance with previous findings (2, 10, 11), torque at failure was linearly related to instrument diameter at D3.

Separation in a cyclic fatigue testing system is believed to occur with the greatest likelihood at the crescent of the curve (18). In the system used in the present study, this point was measured to be at D4 (Fig. 1). However, there was a wide distribution of separated fragment lengths (data not shown). This observation would suggest that manufacturing flaws in some distance to the point of greatest deformation would undergo crack propagation sufficient to ultimately cause instrument separation (17, 19). Moreover, the nonlinear diameter increase for ProTaper instruments may lead to nonlinear effects of prestressing on torsional resistance.

We found that larger instruments, in particular F3, were not only less resistant to cyclic fatigue but were affected most by prestressing. Clinically this would suggest using F3 carefully in curved canals not only to minimize canal transportation but also to reduce the risk of fatigue failure.

It proved difficult to demonstrate a significant effect of prestressing on angle at failure, other than in F3 instruments. Indeed, the Shaper X instrument seemed to have greater angles at failure after being stressed to 90% of the fatigue limit. It is unclear what the reasons for this effect are. Yared et al. reported no change in angle at failure for ProFile instruments (11) and a significant reduction of angle at failure for K3 instruments (10), suggesting an impact of cross-sectional design on the stress distribution (8).

The cyclic fatigue model used in this study resulted in minimal torsional loads ($<$0.08 Ncm) within the stressed instruments. Consequently, the effects on torsional resistance should mainly result from cyclic prestressing.

Scanning electronic micrographs indicated no differences in appearance of instruments after torsional fracture, when new and unstressed instruments were compared. However, fracture surfaces after fatigue failure were different.

In conclusion, build-up of tension within NiTi rotary instruments depends on instrument diameter. Clinically, larger instruments that have been subjected to some cyclic fatigue should be used with great care or discarded.

References

1. Barbakow F, Lutz F. The 'Lightspeed' preparation technique evaluated by Swiss clinicians after attending continuing education courses. Int Endod J 1997;30:46–50.
2. Peters OA, Barbakow F. Dynamic torque and apical forces of ProFile .04 rotary instruments during preparation of curved canals. Int Endod J 2002;35:379–89.
3. Mesgouez C, Rilliard F, Matossian L, Nassiri K, Mandel E. Influence of operator experience on canal preparation time when using the rotary Ni-Ti ProFile system in simulated curved canals. Int Endod J 2003;36:161–5.
4. Thoden van Velzen SK, Duivenvoorden HJ, Schuurs AH. Probabilities of success and failure in endodontic treatment: a Bayesian approach. Oral Surg Oral Med Oral Pathol 1981;52:85–90.
5. Sattapan B, Nervo GJ, Palamara JE, Messer HH. Defects in rotary nickel-titanium files after clinical use. J Endod 2000;26:161–5.
6. Luebke NH, Brantley WA. Torsional and metallurgical properties of rotary endodontic instruments. 2. Stainless steel Gates Glidden drills. J Endod 1991;17:319–23.
7. Gambarini G. Cyclic fatigue of nickel-titanium rotary instruments after clinical use with low- and high-torque endodontic motors. J Endod 2001;27:772–4.
8. Berutti E, Chiandussi G, Gaviglio I, Ibba A. Comparative analysis of torsional and bending stresses in two mathematical models of nickel-titanium rotary instruments: ProTaper versus ProFile. J Endod 2003;29:15–9.
9. Yared GM, Bou Dagher FE, Machtou P. Cyclic fatigue of ProFile rotary instruments after clinical use. Int Endod J 2000;33:204–7.
10. Yared G, Kulkarni GK, Ghossayn F. An in vitro study of the torsional properties of new and used K3 instruments. Int Endod J 2003;36:764–9.
11. Yared G, Kulkarni GK. An in vitro study of the torsional properties of new and used rotary nickel-titanium files in plastic blocks. Oral Surg Oral Med Oral Pathol Oral Radiol Endod 2003;96:466–71.
12. International Organization for Standardisation. Dental root-canal instruments. Part 1: files, reamers, barbed broaches, rasps, paste carriers, explorers and cotton broaches. Geneva; 1992.
13. Haikel Y, Serfaty R, Bateman G, Senger B, Allemann C. Dynamic and cyclic fatigue of engine-driven rotary nickel-titanium endodontic instruments. J Endod 1999;25:434–40.
14. Crump MC, Natkin E. Relationship of broken root canal instruments to endodontic case prognosis: a clinical investigation. J Am Dent Ass 1970;80:1341–7.
15. Al-Fouzan KS. Incidence of rotary ProFile instrument fracture and the potential for bypassing in vivo. Int Endod J 2003;36:864–7.
16. Yared GM, Bou Dagher FE, Machtou P. Failure of ProFile instruments used with high and low torque motors. Int Endod J 2001;34:471–5.
17. McNicholls JL, Brookes PC, Cory JS. NiTi fatigue behaviour. J Appl Phys 1981;52: 7442–4.
18. Pruett JP, Clement DJ, Carnes DL. Cyclic fatigue testing of nickel-titanium endodontic instruments. J Endod 1997;23:77–85.
19. Tobushi H, Hachisuka T, Yamada S, Lin P-H. Rotating-bending fatigue of TiNi shape-memory alloy wire. Mech Mat 1997;26:35–42.

AQ1: Please verify if degrees are correct.